euspen's 23rd International Conference & Exhibition, Copenhagen, DK, June 2023
www.euspen.eu

# A systematic comparison between green and infrared laser for laser powder bed fusion of pure copper through a benchmark artefact

W.E. Alphonso[1] , M. Bayat[1] , V.K. Nadimpalli[1] , J.H.Hattel[1]

[1]*Department of Mechanical Engineering, Technical University of Denmark*

*wayeal@dtu.dk*

**Abstract**
Laser Powder Bed Fusion (L-PBF) is one of the well-established Metal Additive Manufacturing (MAM) technology that is highly applied in aerospace, medical and automotive industries due to its advantages such as high design freedom and low tooling cost. A new generation of heat exchangers and electrical coils with complex geometries can be imagined if pure copper parts can be effectively fabricated using L-PBF. However, producing pure copper parts with no defects by L-PBF is a challenge due to the low optical absorptivity of pure copper to infrared radiation and its high thermal conductivity. To produce dense copper parts the power of the infrared laser (available in most commercial L-PBF machines) must be increased above 400W which can strain the optics of the laser system. Using a green laser instead of an infrared laser is another solution as copper has a high optical absorptivity at this wavelength. In this work, a benchmark artefact with features relevant to thermal management and electromagnetic applications was printed with two state-of-the-art commercial L-PBF systems, each equipped with either an infrared or green wavelength laser. A thorough geometrical investigation was conducted on the benchmark artefacts, and it was concluded that the pure copper artefact manufactured by the green laser system had a higher geometrical accuracy and included minimal defects compared to the artefact produced by the infrared laser.

Laser Powder Bed Fusion, green laser, infrared laser, pure copper, electrical coils, heat exchangers

## 1. Introduction

L-PBF has gained a lot of attention in the last decade from the aerospace, medical, and automotive industries due to its advantages such as part weight reduction, low material waste, high design freedom, consolidation of assemblies, low tooling cost, and digitalization of the manufacturing process chain [1]. Pure copper is used in electrical coils and thermal management devices due to its high intrinsic conductivities and is commonly manufactured by conventional methods which have limited the design freedom and therefore the performance of such devices. The next generation of heat exchangers and electrical coils with complex shapes can be foreseen if defect-free pure copper parts can be manufactured using L-PBF. Production of pure copper parts by L-PBF is a challenge due to copper's thermal properties, which make the material appealing for thermal applications, and also the lower optical absorptivity in the infrared spectra [2]. The high thermal conductivity of pure copper hinders the successful melting of the powder layers as the absorbed thermal energy is conducted away from the melt pool, which leads to a lack of fusion porosities in the final part and results in loss of mechanical and thermal performance. Furthermore, the low absorptivity of pure copper to infrared laser wavelength creates an issue with the effective laser energy absorbed by the powder bed, which leads to the generation of pores in the final part. Most of the commercial state-of-the-art L-PBF machines use an infrared laser which is compatible with non-reflective metals like steel, inconel, titanium, and aluminum [3]. Research has been conducted in recent years to address these issues and successfully produce pure copper parts using L-PBF. Three potential solutions have been identified: either increasing the infrared laser's power to 400W or higher [4], changing the laser's wavelength to the green [5] spectrum or changing the composition of the powder by coating or alloying [6] so that the optical absorptivity is improved in the infrared spectra. According to the authors' knowledge, very limited research has been conducted on using green laser systems for producing pure copper parts, but no research has been done on benchmarking L-PBF machines equipped with infrared and green laser systems for pure copper. Therefore, in this work, a geometrical investigation was conducted on a benchmark artefact produced by green and infrared L-PBF systems in pure copper.

## 2. Methodology

To understand the design limitations of pure copper parts produced by a green and infrared L-PBF system, a benchmark artefact was designed that included features that could potentially be used in applications where L-PBF as a manufacturing method can be beneficial to increase the performance and functionality of products. The benchmark artefact was designed in a modular fashion such that multiple coupons for mechanical, metallurgical, and chemical tests could be easily cut out using wire Electrical Discharge Machining (EDM) as shown in **Figure 1**. The artefact also needs to have a small volume (35 mm x 35 mm x 28 mm) to minimize powder consumption and can be printed in a short build time.

After designing the benchmark artifact, it was printed in pure copper using a commercial EOS M290 L-PBF machine which has an infrared laser, and a Trumpf TruPrint 1000 machine which has a green laser. Two inspection techniques, optical fringe projection, and X-ray Computer Tomography were applied to describe the overall geometrical accuracy of the benchmark artefact and the accuracy of micro-sized internal features, respectively, to assess the quality of the L-PBF-produced artefact. Below is a description of the characterization method and the measurement plan.

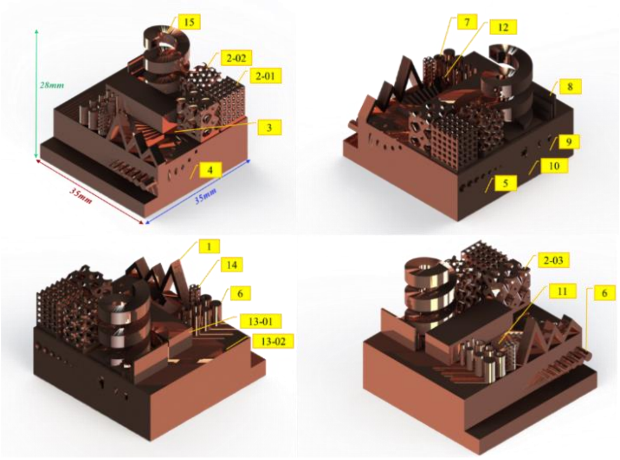


**Figure 1.** Benchmark artefact with different views (a-d) and 15 distinct features tagged with a label.

### *2.1. Optical Fringe Projection*

The geometrical characterization of the entire benchmark artefact was conducted using an optical fringe projection method using a 3Shape optical scanner which was selected as the measurement tool because of its shorter scan times, small measurement volume, and low measurement uncertainty. From this measurement technique, a direct comparison can be made between the nominal geometry and the printed benchmark artefact. The benchmark artefact was adhered to a magnetic plate using clay as a temporary adhesive and the plate was later placed into the measurement volume after calibrating the scanner. A measurement plan was created where the number of orientations at which the benchmark is scanned is selected. Due to the geometric complexity of the artefact, the number of orientation angles for the acquisition was set to 80 orientations (8 swing angles) where 1 swing angle equals 10 rotations. If the number of orientation angles was increased further not much improvement in the quality of the scan was witnessed but the storage size of the file increased. Hence, with this measurement plan, a satisfactory quality of the scanned geometry was obtained. The output of the measurement is a mesh file that was post-processed to delete unwanted regions like the clay used to adhere to the artefact and the surfaces were made smooth using inbuilt filters.

### *2.2. X-ray Computer Tomography (X-ray CT)*

This measurement technique was adopted because it has the benefit of characterizing interior features that are challenging to assess without destroying the artifact. In this technique, the sample was positioned between an x-ray source and a receiver sensor, rotated around a vertical axis, and exposed to x-ray radiation. A collection of 2D tomographs were produced using the receiver sensor's capture of greyscale intensity images at various angular orientations. From this stack of 2D tomograms, a 3D volume was reconstructed by an image processing software after the tomograms were filtered, aligned with a global coordinate system, and binarized using a manual thresholding method. The voxel size used in the investigation of internal channels was 14.48 µm and an exposure time of 4 seconds was implemented.

A ZEISS XRadia 520 Versa equipment was used in this investigation where the instrument was operated at 160 kV and 10 W with a Large Field of View (LFOV) objective and 4X objective along with an HE6 filter. The voxel size was obtained based on the specimen dimensions and after a 2x2 binning. The integrated acquisition and reconstruction software package offered by ZEISS, which is based on a Feldkamp, Davis, and Kress - method using filtered back-projection, was used to conduct the image reconstruction. The features in the benchmark artefact that consisted of internal features like straight and inclined channels were recorded with 4501 projections and stitched together. A high number of projections were required due to the low transmission through the copper bulk sample.

## 3. Results

Once the benchmark artefacts were printed by their respective L-PBF systems, they were cut from the build plate using wire EDM and are shown in **Figure 2** in the as printed condition. The results from the geometrical characterization methods described in the methodology are shown and discussed in this section.

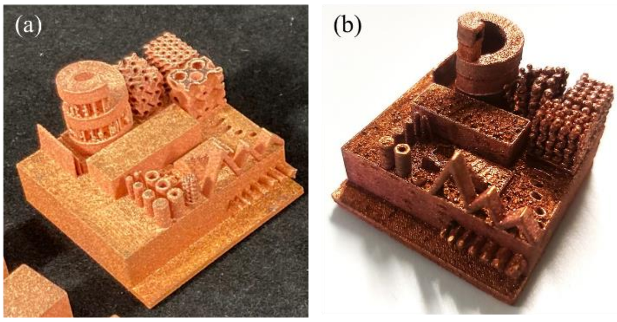


**Figure 2.** Benchmark artefact produced by (a) Green laser – TruPrint 1000 (b) Infrared laser – EOS M290

### *3.1. Optical Fringe Projection*

To get a comprehensive understanding of the dimensional accuracy of the pure copper artefacts made by infrared and green L-PBF systems, the optical fringe projection method was used. After scanning the artefact an STL file of the scanned geometry is imported into GOM Inspect and oriented with the CAD geometry to create a surface deviation plot where the CAD geometry is treated as the nominal geometry. The surface deviation of the benchmark artefact produced by the green and infrared laser systems are shown in **Figure 3** and **Figure 4** respectively. A list of detailed common observations made for different features of the green and infrared laser artefacts that could be detected by this method is shown in **Table 1**.

**Table 1.** Qualitative assessment of features in the benchmark artefact

| Feature | Common observations |
|---|---|
| Triangular overhangs | Dross formation near the triangular vertex on the down-skin for all overhang structures |
| TPMS structures | Macro deviations at the down-skin of all the TPMS structures |
| Straight angular channels | Dross formation on the top surfaces of the channels with the 75° channel affected the most |
| Straight horizontal channels | Dross formation on the top surfaces of the channels and clogged channels for diameter less than 1.25 mm |
| Vertical cylinders | Macro deformation only for cylinder with diameter less than 0.75 mm and 3.5 mm height |
| Horizontal cylinders | Macro deformations after support removal and dimensional inaccuracy for cylinders with diameter less than 0.75 mm and length of 5 mm |
| Thin vertical walls | Bending of all thin walls in the same direction |

| | |
|---|---|
| Double helical fractal and circular channels | Dross formation at the channel inlet |
| 2.5 D Fractal | Reduction inaccuracy near sharp edges and close features when minimum distance is below 0.9 mm |
| Thin pyramids | Macro deviations near sharp edges |
| Helical coil | Macro deviation near the top surface and irremovable support structures |

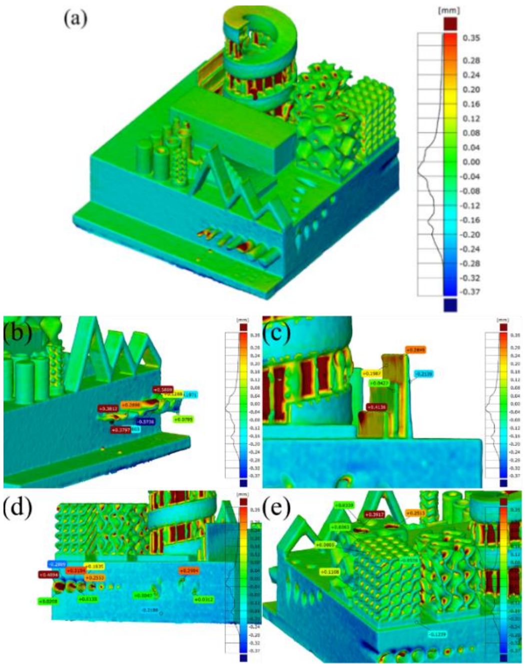

**Figure 3.** Surface deviation plot comparing the nominal geometry with the actual benchmark geometry produced using a green laser system (a) full iso-metric view (b-e) zoomed views

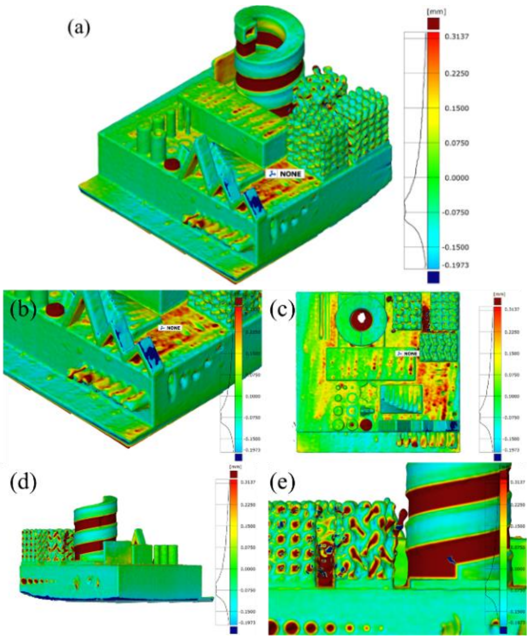

**Figure 4.** Surface deviation plot comparing the nominal geometry with the actual benchmark geometry produced using a infrared laser system (a) full iso-metric view (b-e) zoomed views

Due to the high laser power required by the infrared L-PBF system, several features with high aspect ratios, like thin walls, lattices, and vertical pins, could not be produced. The use of laser power close to 400W and a small beam size of 100 µm can cause overheating issues when printing thin features which can mechanically weaken the features to external loads during the powder coating process. These forces generated by the high aspect ratio features can cause them to fracture easily during the powder coating process when the recoater blade moves across the build plate. The breakage of such features occurs more occasionally as pure copper has a low tensile strength compared to other metals commonly produced using L-PBF. The powder surrounding the region that has been selectively melted also adheres to the melt pool as a result of the overheating, increasing the volume of the feature which is undesired. To compensate for this effect, allowances can be added to the CAD geometry before printing and this can be a part of a Design for Additive Manufacturing (DFAM) guideline for designers who develop pure copper parts that will be manufactured by L-PBF.

Numerous features of the green laser artefact, including those with high aspect ratios like the thin walls and lattices, were successfully printed, but the issue with overheating still exists. The green laser system uses a 485 W laser with a 200 µm laser spot size which results in a larger heating area that leads to the generation of dross defects at the down-skin regions of the lattices and internal channels. Additionally, the 200 µm broad laser beam created large variances in the fractal feature which had a spatial resolution lower than the laser spot size. Additionally, the process parameters selected for the infrared laser generate a keyhole melting mode, whereas the green laser generates a conduction melting mode which has a higher process stability [2].

A green laser system is therefore preferable to an infrared laser system for printing small details and high aspect ratio features, according to the artefacts' optical fringe measurements. By shrinking the spot size of the green laser beam, it is possible to increase the resolution of the features and reduce dross issues on the down skins of internal channels which are formed due to heat accumulation.

### *3.2. X-ray Computer Tomography (X-ray CT)*

The results of the optical fringe projection method demonstrate that the infrared laser artefact is of lower geometrical quality than the artefact produced by the green L-PBF system. As a result, the X-ray CT analysis solely investigates the internal features of the green laser artefact. The modular artefact was split into smaller measurement volumes using wire EDM because the entire benchmark artefact (35 mm x 35 mm x 28 mm) would occupy a too-large measurement volume for a meaningful X-ray CT analysis. The density of pure copper and the size of the features had an impact on the measurement strategy.

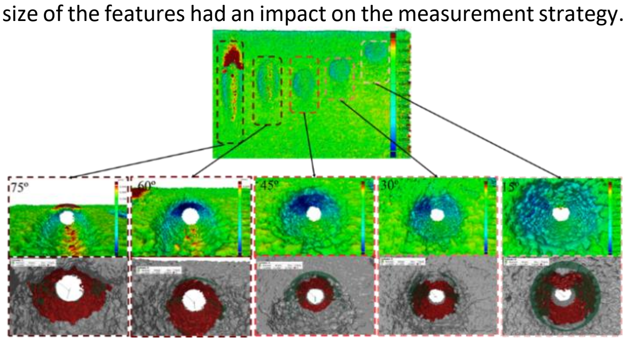

**Figure 5** Surface deviation plot comparing the nominal geometry with the actual benchmark straight channel features with the inclined angles ranging from 15° to 75° to the building direction

Straight angular channels with a theoretical diameter of 1 mm were scanned and oriented with the nominal CAD geometry in GOM inspect to obtain the surface deviation plot as shown in

**Figure 5**. Dross develops on the top surface of the channels when the axis of the straight channels is inclined at an angle less than 45° angle to the building direction. The 75° angular channel's outer vertical wall is deformed as a result of overheating brought on by a relatively thin wall thickness. Using a Gaussian best-fit method, the diameter of each channel is measured, and the relative error to the nominal diameter is computed with the results displayed in **Table 2**. The Gaussian best-fit cylinders for each channel are shown in **Figure 5** and are indicated by a dark green colored cylinder.

**Table 2** Measured diameter of inclined internal straight channels from X-ray CT and calculated relative error to the nominal diameter of 1mm

| Inclination Angle (°) | Gaussian best fit diameter (mm) | Error (%) |
|---|---|---|
| 75 | 1.141 | -14 |
| 60 | 1.197 | -20 |
| 45 | 1.205 | -20 |
| 30 | 1.151 | -15 |
| 15 | 1.136 | -14 |

The measured channel diameter and build orientation do not directly correlate, as evidenced by the computed relative error in **Table 2**. Additional data post-processing will be used in future investigations [7] to characterize the surface roughness inside the channels. On the upper surface of every horizontal channel, whose diameter ranges from 0.5 to 2 mm, dross builds up. The overheating effect due to heat accumulation which is a typical phenomenon in L-PBF [7] results in the formation of dross on the down skin areas, resulting in the clogging of channels with a diameter less than 0.75 mm as shown in **Figure 6**.

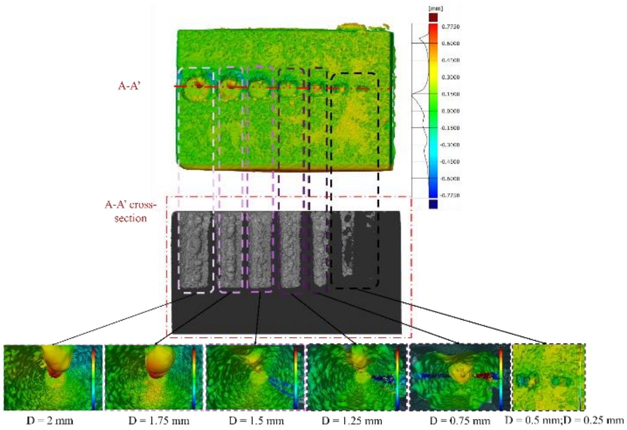


**Figure 6** Surface deviation plot comparing the nominal geometry with the actual benchmark straight horizontal channel features along with a cross sectional view which indicates clogged channels for diameters less than 0.75 mm.

A critical location with a minimum wall thickness of 0.5 mm causes the first channel, which has a 2 mm diameter, to become distorted as a result of heat accumulation. The optical fringe projection of the complete benchmark artefact also captures the sidewall and channel distortion. When compared to the channels printed in 17-4 PH stainless steel, the dross that forms on the down-skin surface of pure copper channels has a different morphology [8]. While the dross in the 17-4 PH channels is coarser and discontinuous, the dross in pure copper channels is smoother and continuous over the length of the channel. The morphology and surface characteristic of the dross differs because of the varied thermophysical properties of the two materials. To eliminate such defects in the printed part, alterations to the nominal channel geometry are needed to compensate for this effect either by changing the shape of the channel from circular or changing the diameter. The degree of allowance in the nominal geometry varies with the selected process parameters, the diameter of the channel, and its orientation to the build direction.

## 4. Summary

In this work, a geometrical investigation of a novel modular benchmark artefact produced by a green and infrared L-PBF system in pure copper was completed. The accuracy of the printed external and internal features of the benchmark artefact was determined using optical fringe projection and X-ray CT methods, respectively. The results showed that the artifact created with the green laser system was significantly better than the artifact created with the infrared laser system. This is because pure copper has a high optical absorptivity in the green wavelength and the laser system's 200 µm beam size creates a conduction melting mode which increases the process stability. The X-ray CT measurement of the straight angular internal channels showed that the actual diameter is larger than the nominal diameter for all inclinations. The X-ray CT of the horizontal channels showed that the channels which have a diameter smaller than 0.75 mm are clogged due to excessive dross formation. Future work should include a more in-depth surface characterization of the internal inclined and horizontal channels. Preparing and publishing DFAM guidelines for pure copper parts manufactured by green laser L-PBF system will also be a part of future work.

## References


1] L. Jyothish Kumar, P. M. Pandey, and D. I. Wimpenny, *3D printing and additive manufacturing technologies*. Springer Singapore, 2018. doi: 10.1007/978-981-13-0305-0.

[2] S. Engler, R. Ramsayer, and R. Poprawe, “Process studies on laser welding of copper with brilliant green and infrared lasers,” *Phys Procedia*, vol. **12**, no. PART 2, pp. 339–346, 2011, doi: 10.1016/j.phpro.2011.03.142.

[3] H. Siva Prasad, F. Brueckner, J. Volpp, and A. F. H. Kaplan, “Laser metal deposition of copper on diverse metals using green laser sources,” *International Journal of Advanced Manufacturing Technology*, vol. **107**, no. 3–4, pp. 1559–1568, 2020, doi: 10.1007/s00170-020-05117-z.

[4] S. D. Jadhav, L. R. Goossens, Y. Kinds, B. van Hooreweder, and K. Vanmeensel, “Laser-based powder bed fusion additive manufacturing of pure copper,” *Addit Manuf*, vol. **42**, no. March, 2021, doi: 10.1016/j.addma.2021.101990.

[5] S. Gruber, L. Stepien, E. López, F. Brueckner, and C. Leyens, “Physical and geometrical properties of additively manufactured pure copper samples using a green laser source,” *Materials*, vol. **14**, no. 13, 2021, doi: 10.3390/ma14133642.

[6] V. Lindström *et al.*, “Laser powder bed fusion of metal coated copper powders,” *Materials*, vol. **13**, no. 16, 2020, doi: 10.3390/MA13163493.

[7] C. G. Klingaa, T. Dahmen, S. Baier-Stegmaier, S. Mohanty, and J. H. Hattel, “Investigation of the roughness variation along the length of LPBF manufactured straight channels,” *Nondestructive Testing and Evaluation*, vol. **35**, no. 3, pp. 304–314, Jul. 2020, doi: 10.1080/10589759.2020.1785445.

[8] C. G. Klingaa, T. Dahmen, S. Baier, S. Mohanty, and J. H. Hattel, “X-ray CT and image analysis methodology for local roughness characterization in cooling channels made by metal additive manufacturing,” *Addit Manuf*, vol. **32**, no. February, p. 101032, 2020, doi: 10.1016/j.addma.2019.101032.